

Supporting information

The Effect of Injection Routes on the Biodistribution, Clearance and Tumor Uptake of Carbon Dots

Xinglu Huang,[†] Fan Zhang,^{†,‡} Lei Zhu,^{†,‡} Ki Young Choi,[†] Ning Guo,[†] Jinxia Guo,^{†,‡} Kenneth Tackett,[¶] Parambath Anilkumar,[¶] Gang Liu,[‡] Qimeng Quan,[†] Hak Soo Choi,[§] Gang Niu,[†] Ya-Ping Sun,[¶] Seulki Lee,[†] Xiaoyuan Chen^{†*}

[†]Laboratory of Molecular Imaging and Nanomedicine (LOMIN), National Institute of Biomedical Imaging and Bioengineering (NIBIB), National Institutes of Health (NIH), Bethesda, Maryland, 20892, United States

[‡]Center for Molecular Imaging and Translational Medicine, School of Public Health, Xiamen University, Xiamen 361005, China

[¶]Department of Chemistry and Laboratory for Emerging Materials and Technology, Clemson University, Clemson, South Carolina 29634, United States

[§]Division of Hematology/Oncology, Department of Medicine, Beth Israel Deaconess Medical Center, Boston, Massachusetts 02215, United States

*Corresponding Author: e-mail; Shawn.Chen@nih.gov

METHODS

Instruments

Transmission electron microscope (TEM) images were obtained on FEI Tecnai 12 electron microscope operated with an acceleration voltage of 120 kV. Zeta potential of the particles was measured using a SZ-100 nanoparticle analyzer (Horiba Scientific). The UV-Vis and fluorescence spectra of particles were recorded on a Genesys 10s UV-Vis spectrophotometer (Thermo, IL) and an F-7000 fluorescence spectrophotometer (HiTachi, Japan), respectively. Positron emission tomography (PET) scans were evaluated with an Inveon preclinical PET scanner (Siemens Medical Solutions). The radioactivity of organs was measured using a γ -counter (1480 Wizard 3; PerkinElmer). Tissue slides were examined by an Olympus IX81 fluorescence microscopy. Fluorescence images of C-dots solutions and live animals were acquired using a Maestro fluorescence imaging system (PerkinElmer, MA). The filter set of the Maestro imaging system was listed as below.

Maestro Filter Set Name	Excitation Filter	Emission Filter	Acquisition Settings
White	Neutral attenuator	Transparent glass filter	500 to 800 in 10 nm steps
Blue	455 nm (435 to 480 nm)	490 nm longpass	500 to 720 in 10 nm steps
Green	523 nm (503 to 548 nm)	560 nm longpass	560 to 750 in 10 nm steps
Yellow	595 nm (576 to 621 nm)	635 nm longpass	630 to 800 in 10 nm steps
Orange	605 nm (586 to 601 nm)	645 nm longpass	640 to 820 in 10 nm steps
Red	635 nm (616 to 661 nm)	675 nm longpass	670 to 900 in 10 nm steps
Deep Red	661 nm (641 to 681 nm)	700 nm longpass	700 to 950 in 10 nm steps
NIR	704 nm (684 to 729 nm)	745 nm longpass	740 to 950 in 10 nm steps

To demonstrate the low tissue absorption and scattering of particles in the NIR emission window, a low concentration of C-dot-ZW800 (6.25 $\mu\text{g/mL}$) in different biological fluids (PBS, fetal bovine serum, mouse blood, mouse urine and kidney tissue lysate) was imaged using a Maestro imaging system (Filter set, NIR). For the preparation of tissue lysate derived from kidney, mice were sacrificed and the kidneys were isolated. The kidneys were wet-weighted and homogenized in 0.5 mL of lysis buffer (0.25 M sucrose, 40 mM Tris acetate, 10 mM EDTA) with a T10 basic ULTRA-TURRAX homogenizer (IKA). After strong vortex, 1 mL of extraction solution (0.75 M HCl in IPA) was added and the samples were incubated at -20 $^{\circ}\text{C}$ overnight. After centrifugation at 24,000 g for 15 min, the supernatant was stored for further use. The results showed that the biological medium had low background in the NIR region, without significantly affecting the fluorescence intensity of particles.

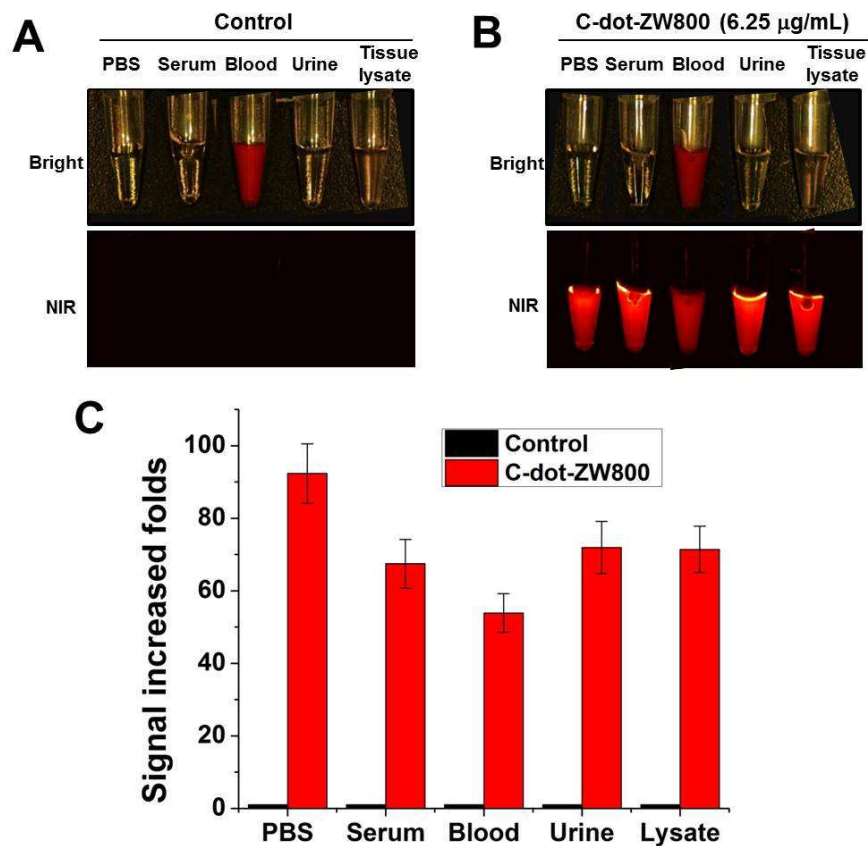


Figure S1. Fluorescence images of different biological fluids (A) without and (B) with the presence of C-dot-ZW800 particles. (C) Quantification of fluorescence signal of C-dot-ZW800 in PBS, mouse serum, blood, urine and kidney lysate.

To explore the fluorescence stability of particles, the C-dot-ZW800 was diluted in biological fluids (6.25 $\mu\text{g/mL}$), including mouse urine and mouse vein blood. Then, the fluorescence stability of C-dot-ZW800 was observed using a Maestro imaging system (Filter set, Blue and NIR). The results demonstrated the fluorescence signal of particles was virtually unaltered over extended incubation time.

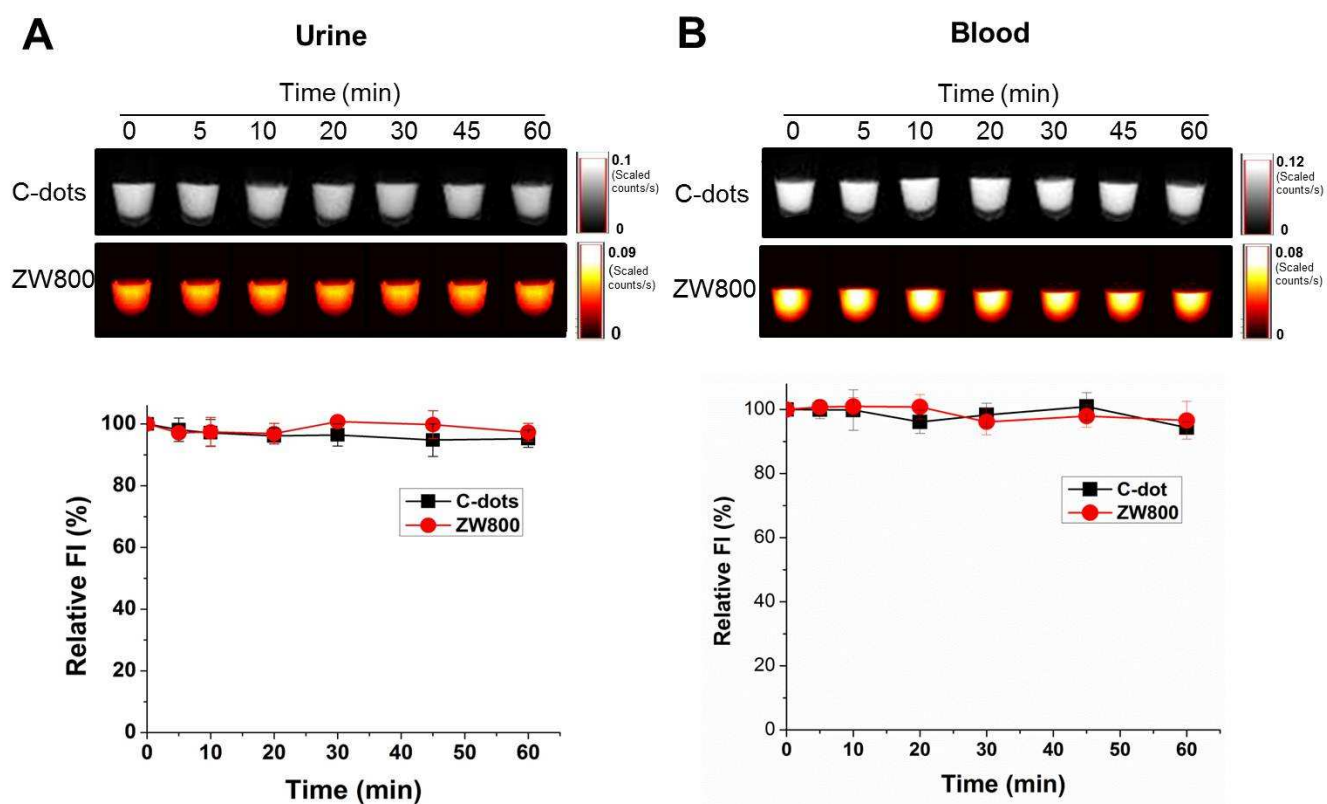


Figure S2. Fluorescence stability of particles in (A) urine and (B) blood at 37 °C over time. Top, fluorescence imaging of C-dot-ZW800 over time; Bottom, quantification of fluorescence intensity of particles.

Tissue sample collection and analysis. Animal procedures were performed according to a protocol approved by the National Institutes of Health Clinical Center Animal Care and Use Committee (NIH CC/ACUC). After the injection of C-dot-ZW800, different organ and tissue samples were collected and analyzed. Briefly, C-dot-ZW800 in PBS solution (2.5 mg/kg, 50 μ L) were injected by different routes (n = 4/group): intravenous injection (i.v., tail vein), subcutaneous injection (s.c., under the skin of left leg), and intramuscular injection (i.m., muscle of left leg), respectively. Blood samples (5 μ L/withdrawal) were collected from tail vein at different time points (1, 2, 5, 10, 15, 20, 25, 30, 45, and 60 min) postinjection of C-dot-ZW800. The samples were analyzed by a Maestro all-optical imaging system (Filter set, Blue and NIR). The results showed the same trend of blood clearance for C-dots and ZW800, demonstrating that the conjugated ZW800 dye molecules were not removed from the C-dot particles (Fig. S3). The accumulation of particles at injection sites was also studied by exposing injection sites after different routes of injection and then imaged by a Maestro all-optical imaging system (Filter set, NIR).

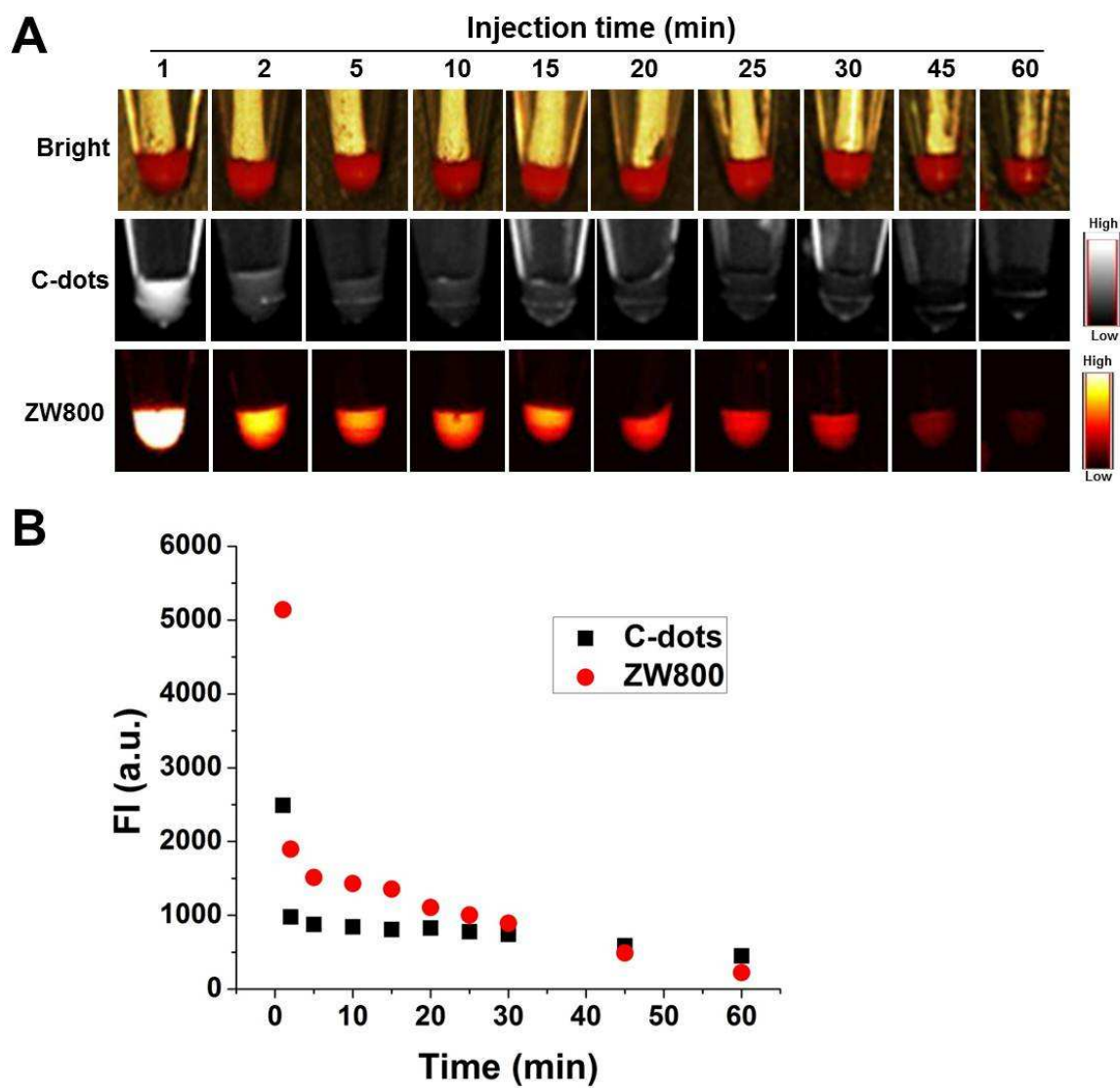


Figure S3. Imaging of blood samples over time after i.v. injection (top, bright field; middle, C-dot fluorescence; bottom, ZW800 fluorescence).

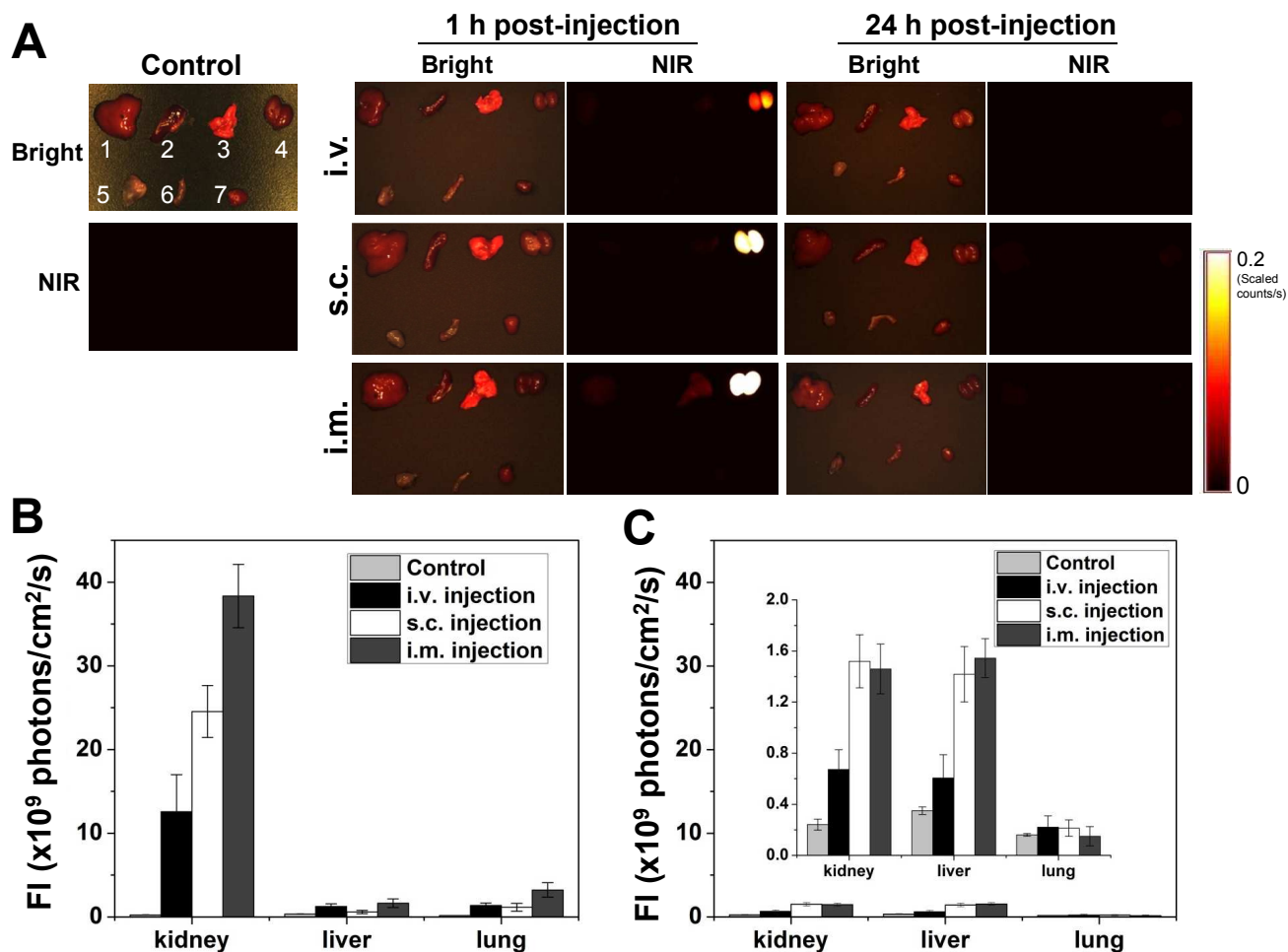


Figure S4. Biodistribution of particles by optical imaging after three injection routes. (A) *Ex vivo* imaging of biodistribution of C-dot particles. After injection of particles, the major organs and tissues were harvested from Balb/C mice at the indicated time points, and subsequently, the bright field and NIR imaging were acquired using a Maestro imaging system. Left, control mice without C-dot injection; middle, 1 h post-injection (top, i.v.; middle, s.c.; bottom, i.m.); right, 24 h post-injection (top, i.v.; middle, s.c.; bottom, i.m.). Bright field: 1, liver; 2, spleen; 3, lung; 4, kidneys; 5, muscle; 6, intestine; 7, heart. (B-C) Quantification of the biodistribution of C-dots in the kidneys, liver and lung *via* three injection routes at 1 h (B) and 24 h (C) time points. The unit of fluorescence signal is $\times 10^9$ photons/cm²/s.

Labeling of C-dots with PET isotope ⁶⁴Cu.

For ^{64}Cu labeling, the amino groups of C-dots were firstly conjugated with DOTA-NHS ester (Macrocyclics, Inc). Briefly, 5 mg C-dots were reacted with 0.5 mg DOTA-NHS ester in 2 ml borate buffer (pH = 9.0). The mixture was stirred at room temperature for 4 h, and subsequently purified by PD-10 desalting column. The product was concentrated into 0.5 mL PBS with a centrifugal filter. Then, the C-dot-DOTA conjugate was labeled with 1 mCi of ^{64}Cu for 1 h in NH_4Ac buffer (pH = 5.4) followed by PD-10 column purification. ^{64}Cu was produced at NIH by the irradiation of a thin layer of ^{64}Ni (Isoflex, USA) electroplated on a solid gold internal target plate of the CS-30 cyclotron utilizing the nuclear reaction $^{64}\text{Ni}(p,n)^{64}\text{Cu}$ and separated from the target material as $^{64}\text{CuCl}_2$ by anion chromatography.

At 1 h and 24 h postinjection of ^{64}Cu -C-dot, the mice were euthanized and major organs and tissues including blood, muscle, liver, kidneys, spleen, heart and lung were harvested and measured by gamma counting.

For the urine clearance analysis, the mice were kept under isoflurane anesthesia (2% v/v isoflurane in $0.2 \text{ L min}^{-1} \text{ O}_2$ flow) and the bladders of mice were exposed. Subsequently, the bladders were imaged before and after three injection routes at indicated time points. Separate animals were also sacrificed and different organs/tissues were collected at different time points for *ex vivo* fluorescence imaging. NIR fluorescence imaging was acquired for ZW800 on a Maestro all-optical imaging system (Filter set, C-dot and NIR).

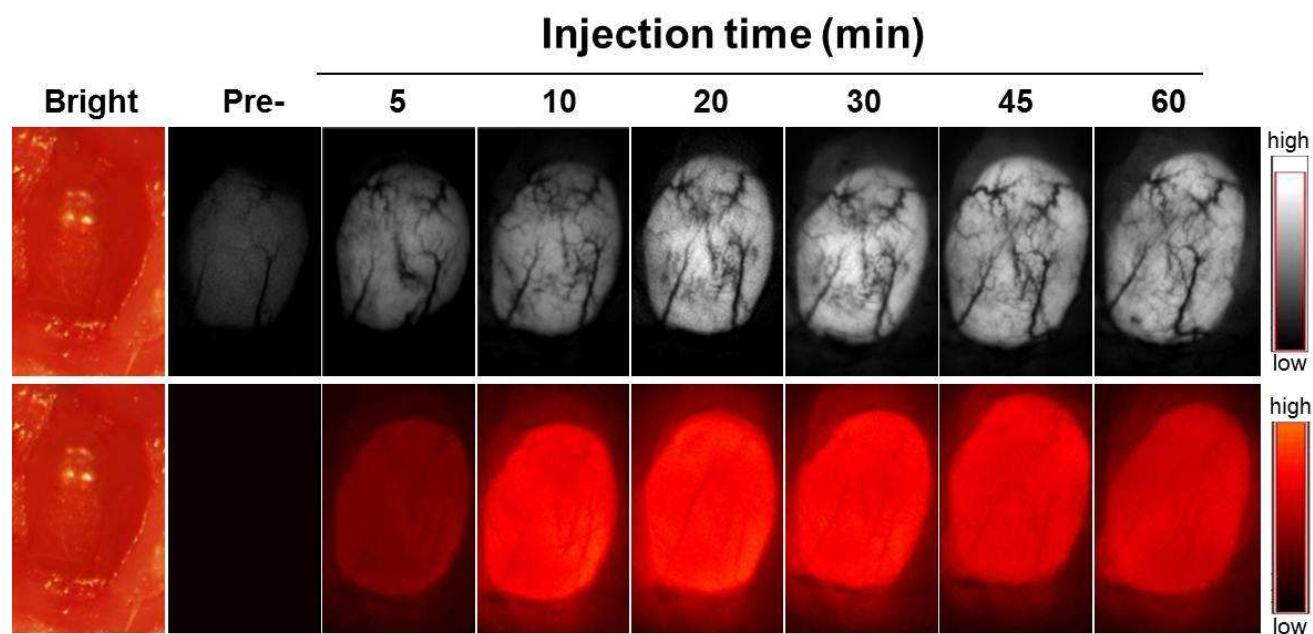


Figure S5. Imaging of urine clearance of C-dot-ZW800 particles in exposed bladder over time by i.v. injection (Left, bright field; top, C-dot fluorescence; bottom, ZW800 fluorescence).